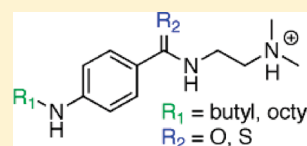# Cyclic Nucleotide-Gated Channel Block by Hydrolysis-Resistant Tetracaine Derivatives

Adriana L. Andrade,[†] Kenneth Melich,[†] G. Gregory Whatley,[‡] Sarah R. Kirk,[‡] and Jeffrey W. Karpen*,[†]

[†]Program in Chemical Biology, Department of Physiology and Pharmacology, Oregon Health & Science University, 3181 SW Sam Jackson Park Road, Portland, Oregon 97239, United States

[‡]Department of Chemistry, Willamette University, Salem, Oregon 97301, United States

ABSTRACT: To meet a pressing need for better cyclic nucleotide-gated (CNG) channel antagonists, we have increased the biological stability of tetracaine-based blockers by synthesizing amide and thioamide linkage substitutions of tetracaine (**1**) and a higher affinity octyl tail derivative (**5**). We report the apparent K_D values, the mechanism of block, and the in vitro hydrolysis rates for these compounds. The ester linkage substitutions did not adversely affect CNG channel block; unexpectedly, thioamide substitution in **1** (compound **8**) improved block significantly. Furthermore, the ester linkage substitutions did not appear to affect the mechanism of block in terms of the strong state preference for closed channels. All ester substituted compounds, especially the thioamide substitutions, were more resistant to hydrolysis by serum cholinesterase than their ester counterparts. These findings have implications for dissecting the physiological roles of CNG channels, treating certain forms of retinal degeneration, and possibly the current clinical uses of compound **1**.

INTRODUCTION

Cyclic nucleotide-gated (CNG) ion channels are known for their role in phototransduction in retinal photoreceptors and in odorant transduction in the olfactory epithelium.[1,2] CNG channels are also present in other brain regions and nonsensory tissues, but their physiological roles are much less clear.[3−7] CNG channel activation in photoreceptors is regulated by the cytoplasmic concentration of cGMP, which binds to and opens the channel to allow influx of Na^+ and Ca^{2+} ions. Alterations of CNG channel activity have been observed in some forms of retinitis pigmentosa, a group of inherited diseases that cause progressive degeneration of rod and cone photoreceptors.[8−14] Mutations that cause elevated cGMP levels lead to prolonged channel activation and Ca^{2+}-triggered cell death.[10,12,14−17] In mouse models, reduction of CNG channel activity strongly correlated with improvements in the overall progression of the disease[18−20] (see also refs 21 and 22), but unfortunately, there are no clinically approved drugs that target CNG channels.

Compared to voltage-gated channels, CNG channel pharmacology is quite unsophisticated.[20,23] The most widely used CNG channel antagonist in research, *l-cis*-diltiazem, is an incomplete blocker and relatively nonspecific.[24−27] CNG channels are also blocked by some local anesthetics, one example being tetracaine [2-(dimethylamino)ethyl 4-(butylamino)benzoate] (**1**).[28−30] Compound **1** blocks CNG channels with relatively high affinity, although differently from voltage-gated sodium channels. Like sodium channels, the interaction of **1** with CNG channels is thought to be in the selectivity filter and the pore region.[31−35] However, **1** has a greater affinity for the sodium channel in its open, inactivated-state,[36] whereas for CNG channels, it binds with higher affinity to the closed state.[37] The inability of **1** and *l-cis*-diltiazem to distinguish between CNG channels and other channels leads to the conclusion that much research remains to be done on better CNG channel antagonists.

In recent years, our group has developed a number of high affinity CNG channel blockers using **1** as a scaffold.[38−40] Compound **1** is clinically approved for temporary anesthesia in various surgical procedures, including those involving the eye.[41,42] Its effects are localized and short-lived because of its rapid degradation by esterases.[43] One major improvement in the design of a tetracaine-based CNG channel blocker would be to increase its biological stability against hydrolysis. In this study, we have synthesized amide and thioamide linkage versions of **1**, as well as its relative **5** that has a higher affinity for CNG channels.[40] We report the apparent K_D values and in vitro hydrolysis rates by serum cholinesterase (butyrylcholinesterase) for these novel compounds. We believe we have uncovered promising compounds not only for CNG channel research but for the treatment of specific forms of retinal degeneration as well. Furthermore, these improvements may have implications for current clinical usage of **1** in general.

CHEMISTRY

Compound **1** derivatives were prepared according to Scheme 1. An alkyl substituent was added to the amino end of 4-aminobenzoic acid (**2**) via reductive amination using a synthesis adapted from Sato et al.[44] The resulting alkylated benzoic acid derivatives (**3** and **4**) were then activated at the carboxylic acid with 1,1′-carbonyldiimidazole (CDI) and subsequently esterified or amidated using 2-(dimethylamino)ethanol or N′,N′-dimethylethane-1,2-diamine, respectively, to yield target compounds

Scheme 1. Synthesis of Tetracaine Derivatives[a]
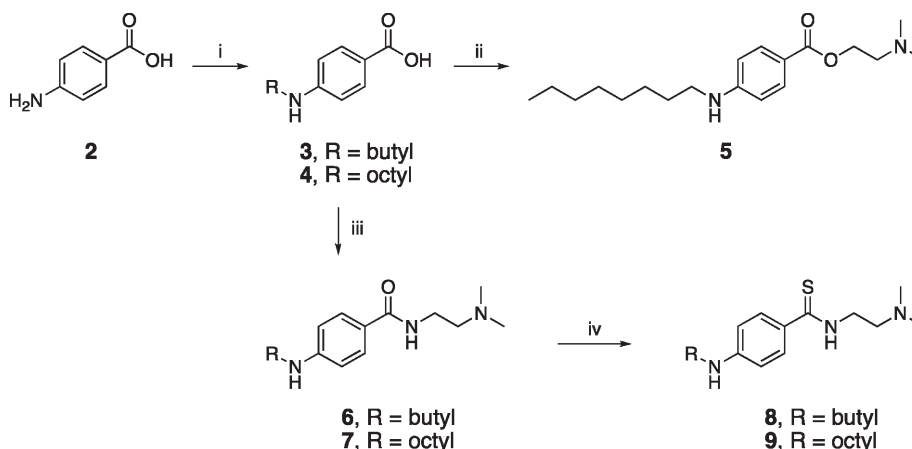
[a] Reagents and conditions: (i) butanal or octanal, α-picoline-borane, MeOH, room temp, 16—24 h (88%, 94%); (ii) CDI, DME, 60 °C, 2 h, followed by 2-(dimethylamino)ethanol, NaH, 60 °C to room temp, 16—24 h (95%); (iii) CDI, DME, 60 °C, 2 h, followed by N′,N′-dimethylethane-1,2-diamine, NaH, 60 °C to room temp, 16—24 h (93%, 87%); (iv) Lawesson's reagent, toluene, reflux, 2.5 h (26%, 73%).

5—7.[45] Compounds **6** and **7** were further treated with Lawesson's reagent to yield target thioamide compounds **8** and **9**.[46]

■ RESULTS

CNG Channel Block at Saturating cGMP. The effectiveness of retinal rod CNG channel current block by the ester linkage-substituted tetracaine derivatives was tested in *Xenopus* oocyte preparations. Excised, inside-out patches pulled from oocytes expressed heteromeric rod CNG channels consisting of CNGA1 and CNGB1 subunits. This was verified by substantial block of 2 mM cGMP-induced currents with 20 μM *l-cis*-diltiazem (74.2 ± 5.8% at $V_m = +50$ mV).[47]

Each compound's apparent affinity for the heteromeric CNG channel was determined under maximal channel activation (2 mM cGMP). CNG channel currents were elicited by a voltage step protocol to −50 and +50 mV (Figures 1A and 2A, insets). The apparent K_D value at each membrane potential was estimated first by determining I_{+B} and I_{-B} at steady state, where I_{+B} is the current in the presence of blocker and I_{-B} is current in the absence of blocker, for different blocker concentrations ([B]). The following equation for block at a single binding site was fit to the data to obtain K_D:

$$I_{+B} = I_{-B}K_D/(K_D + [B])$$

Representative traces for CNG channel currents at positive and negative membrane potentials activated by 2 mM cGMP, as well as graphs with fitted curves, are shown for compounds **1**, **8**, **5**, and **9** in Figures 1 and 2. As reported previously,[40] **5** had a higher affinity for CNG channels than **1** (Figures 1 and 2). Compound **8** proved to be a higher affinity CNG channel blocker compared to compound **1** at both positive and negative membrane potentials (Figure 1). In contrast, compound **9** with the same headgroup linkage as compound **8** had a similar CNG channel affinity compared to compound **5** (Figure 2). From Figures 1A and 2A, it is also possible to note the characteristic voltage dependence of block of compounds **1** and **5**, which improves with positive membrane potentials. All compounds tested exhibited voltage-dependent block, although the voltage-dependence of **5** and its derivatives was appreciably less than that of **1** and its derivatives.

A small transient decay in current attributed to an ion accumulation effect was seen with each voltage step with large currents (typically >1 nA, Figures 1 and 2).[48] Corrections for ion accumulation did not substantially change previous K_D estimates for **1** (6.8 μM corrected for ion accumulation[39] and 6.7 μM not corrected,[40] both determined at +40 mV). We found that the K_D value estimates taking this effect into account did not change the relationship among the compounds for block; hence, it was not corrected for in the values reported here.

The K_D values at both +50 and −50 mV for all compounds tested are plotted in Figure 3. The mean K_D values are summarized in Table 1, along with estimated log P values for each compound. On the basis of these results, it is apparent that the headgroup linkage of **5** has a limited role in CNG channel current block. However, substitutions of the headgroup linkage in **1**, in particular the carbonyl oxygen, play a direct role in CNG channel interaction. While the amide substitution of the ester linkage of **1** (compound **6**) has little effect on the K_D values, the thioamide substitution unexpectedly improves the effectiveness of block (compound **8**).

State Dependence of Block. Compound **1** has been reported to preferentially block CNG channels in the closed conformation, and the effectiveness of block improves with half-maximal channel activation.[37] Although we previously established that **5** has a greater affinity for CNG channels under saturating concentrations of cGMP than **1**, we did not examine if the mechanism of block was different. We sought to determine if the ester linkage-substituted compounds, as well as compound **5**, exhibit state preference for block. We measured the apparent K_D values at both positive and negative potentials for CNG channel currents activated by saturating (2 mM) and subsaturating concentrations of cGMP (50 and 100 μM). Under these conditions, with no exceptions, the determined K_D values for all compounds were smaller at subsaturating cGMP than at saturating cGMP. The K_D values at subsaturating cGMP (at +50 mV) normalized to the K_D values at saturating cGMP are plotted against $1 - I/I_{max}$, which is related to the fraction of closed channels, for compounds **1**, **8**, **5**, and **9** in Figure 4. The solid lines are simulations for the expected relationship between K_D and fraction of closed channels for an exclusive closed channel blocker, using three previously determined estimates for the
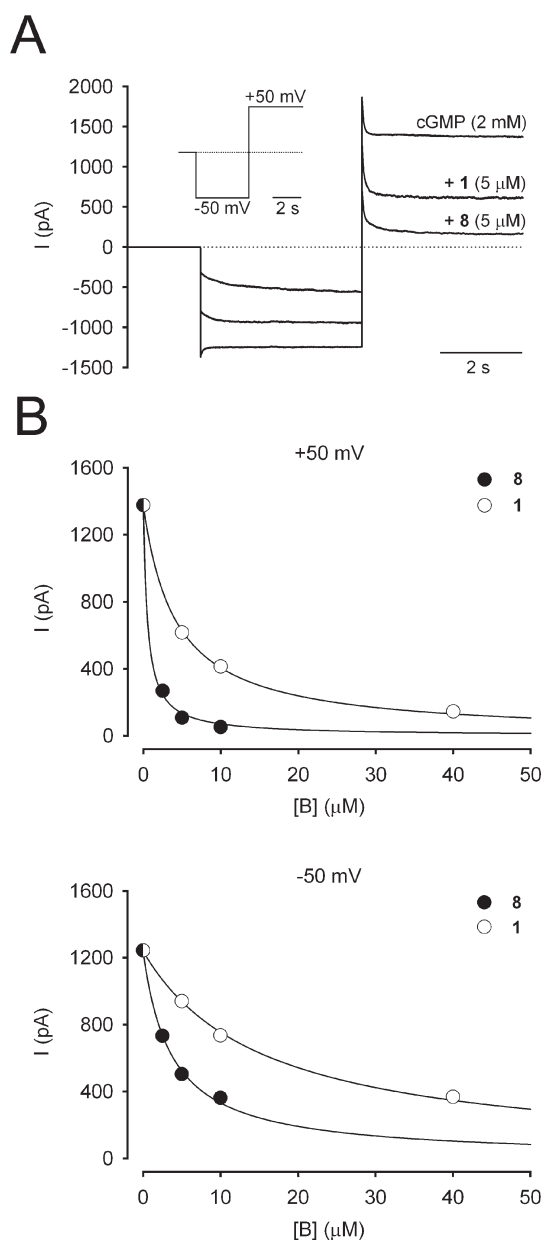
Figure 1. Heteromeric rod CNG channel block by compounds **1** and **8**. Leak-subtracted currents from a representative excised inside-out patch from oocytes expressing heteromeric rod CNG channels (A). Currents were elicited by a voltage step protocol from 0 to −50 to +50 mV (inset) in the presence of 2 mM cGMP or 2 mM cGMP and compound (5 μM). Time scale is shown in the lower left-hand corner of the panel and inset, and the zero current level is indicated by the dotted line. (B) Currents obtained from a concentration series of compounds **1** (white) and **8** (black) are plotted against compound concentration. Solid line indicates the fit of the equation for block at a single binding site (see text). K_D values determined from the fit of the equation were 4.2 μM at +50 mV and 15.6 μM at −50 mV for compound **1**, and 0.5 μM at +50 mV and 3.7 μM at −50 mV for compound **8**.

Figure 2. Heteromeric rod CNG channel block by compounds **5** and **9**. Leak-subtracted currents from a representative excised inside-out patch from oocytes expressing heteromeric rod CNG channels (A). Currents were elicited by a voltage step protocol from 0 to −50 to +50 mV (inset) in the presence of 2 mM cGMP or 2 mM cGMP and compound (5 μM). Time scale is shown in the lower left-hand corner of the panel and inset, and the zero current level is indicated by the dotted line. (B) Currents obtained from a concentration series of compounds **5** (white) and **9** (black) are plotted against compound concentration. Solid line indicates the fit of the equation for block at a single binding site (see text). K_D values determined from the fit of the equation were 1.5 μM at +50 mV and 1.8 μM at −50 mV for compound **5**, and 1.3 μM at +50 mV and 1.8 μM at −50 mV for compound **9**.

probability of closed heteromeric retinal rod channels at saturating cGMP (a−c).[49−51] The dotted line is a simulation for a blocker with no preference for state, while the dashed line is a simulation for an exclusive open channel blocker. Despite inherent variability in the relationships between K_D values and fractional current, the data for all compounds track much better
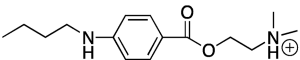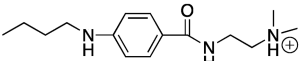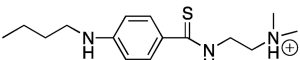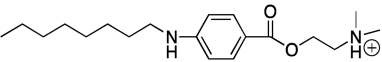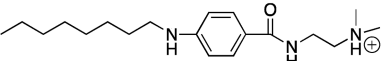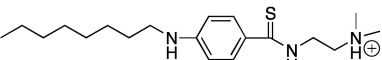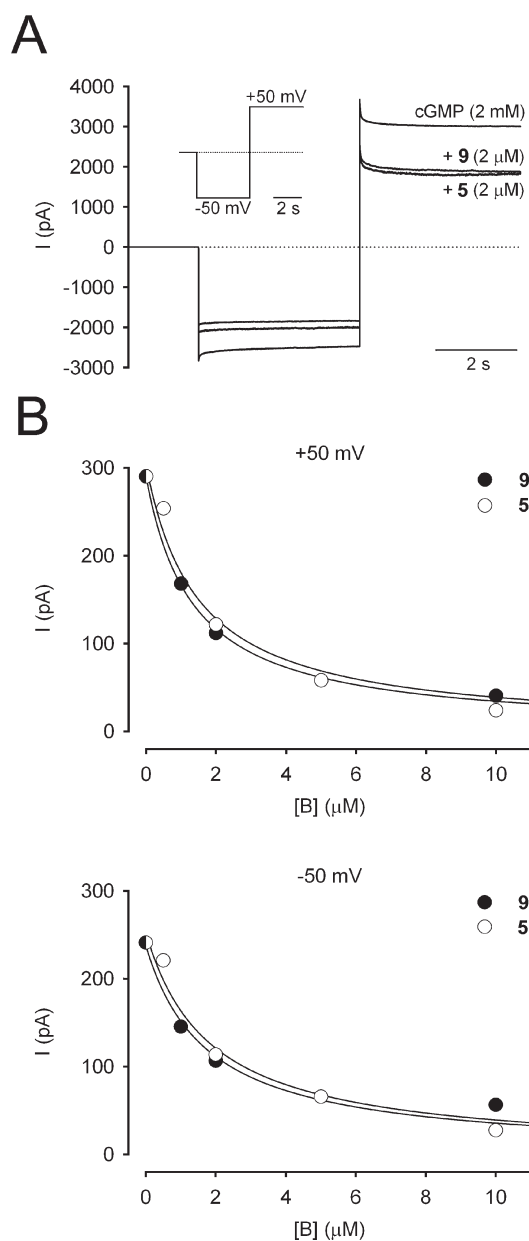
with an expected closed channel blocker. Thus, increasing the butyl tail of compound **1** to eight carbons (compound **5**), as well as substituting the ester linkages of both **1** and **5**, does not appear to alter the essential mechanism of CNG channel block.

Resistance to in Vitro Hydrolysis. In addition to the unexpected increase in apparent affinity for CNG channels by compound **8**, the

Table 1. K_D Value Determinations, Estimated Log P, and in Vitro Serum Cholinesterase Hydrolysis Rates for Tetracaine (1) and Derivatives

Compound[a]	Structure	$K_{D(+50)}$ (μM)	$K_{D(-50)}$ (μM)	n	Log P[b]	Hydrolysis rate nmols.min^{-1}.mg^{-1}
1		4.9 ± 1.8	21.8 ± 8.6	16	3.1	132 ± 10
6		4.4 ± 2.0	28.6 ± 13.1	7	2.3	8.4 ± 3.5
8		0.6 ± 0.3	3.9 ± 1.8	4	2.8	ND[c]
5		1.0 ± 0.6	2.4 ± 1.4	5	5.1	213 ± 31
7		1.6 ± 1.5	3.7 ± 1.5	4	4.3	1.2 ± 0.5
9		0.7 ± 0.5	1.8 ± 0.8	5	4.8	ND[c]

[a] The compounds are shown here in what is expected to be the predominant protonation state at pH 7.6. [b] Calculated for the unprotonated forms using ALOGPS 2.1 (Virtual Computational Chemistry Laboratory). [c] Not detected.

amide and thioamide linkage substitutions should provide an improvement for many in vivo applications or tissue preparations to a tetracaine-based CNG channel blocker in terms of biological stability. Compound 1 is rapidly hydrolyzed by butyrylcholinesterase in the bloodstream,[43] hence, its limitation to local targets in clinical usage. Butyrylcholinesterase is also the predominant esterase present in ocular tissues.[52−54] Similarly, in vivo use of a tetracaine-based CNG channel blocker would be short-lived. Amide and thioamide linkages are more resistant to hydrolysis than ester linkages. We therefore tested the resistance of the ester linkage-substituted compounds to in vitro hydrolysis using butyrylcholinesterase purified from human blood serum (Table 1). The concentrations of compounds used in the assays were well in excess of butyrylcholinesterase's K_m for 1 and other local anesthetics.[43] The amide linkage substitutions of compounds 6 and 7 increased the resistance to hydrolysis substantially. The increase in hydrolysis resistance was even more dramatic for the thioamide linkage substitutions (compounds 8 and 9), which proved to be much too stable for our system to detect any hydrolysis product, even after 24 h incubations.

One concern relating to the amide linkage (compounds 6 and 7) is that it could increase the susceptibility of hydrolysis by proteases present in the eye.[55,56] However, this was not the case. Using the broad-spectrum, nonspecific endopeptidases chymotrypsin and proteinase K, we were not able to detect any hydrolysis products for all compounds, while hydrolysis products of 4-nitrophenyl acetate and BSA were detected as positive controls.

■ DISCUSSION

We have synthesized and determined the apparent affinities and mechanism of CNG channel block, as well as the hydrolysis rates, for four novel tetracaine-based compounds with potentially increased biological stabilities (compounds 6, 7, 8, and 9). The K_D values obtained for 1 and 5 (Table 1) were similar to those previously reported.[39,40] As expected, 5 had a higher apparent affinity for CNG channels than 1. The substituted amide linkages (compounds 6 and 7) did not adversely affect the apparent affinity for CNG channel block (Table 1). In addition, these compounds were more resistant to esterase hydrolysis than their ester counterparts (compounds 1 and 5). This poses a significant advantage for their use in in vivo research or in the clinic.

Compounds 8 and 9 were even more resistant to esterase hydrolysis than compounds 6 and 7, attributed to the thioamide linkage substitution (Table 1). For compound 9 the thioamide substitution did not enhance the apparent affinity for CNG channels, but it did for compound 8. It is unknown why the thioamide substitution in compound 8 improved CNG channel block, as the precise structure of the channel pore remains unresolved. These results suggest that 1 and its derivatives bind at a different site in the channel than 5 and its derivatives. The observation is further supported by the exhibited differences in voltage dependence of block. It is possible that the lower electronegativity or increased size of sulfur in lieu of the carbonyl oxygen enhances the interaction of compound 8, improving the apparent affinity for the channel pore. It is also possible that the presence of sulfur instead of oxygen increases the partial double bond character of the carbon−nitrogen bond, affecting the orientation of the aromatic and headgroup moieties.

Compound 1 has been reported to be a closed-channel blocker.[37] Although we have previously determined the K_D values for 5, its mechanism of block had not yet been examined. Compound 5, as well as all compounds in this study, exhibited preference for the closed state over the open state (Figure 4).
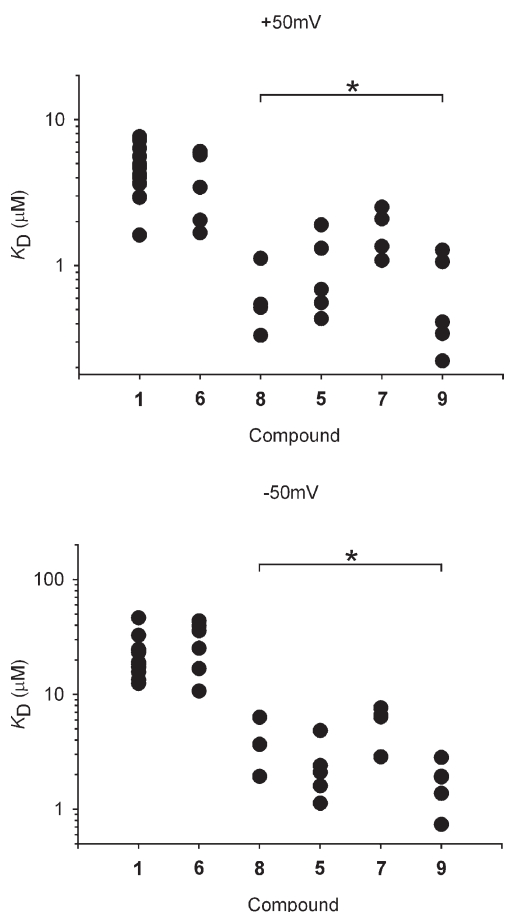
Figure 3. K_D values determined from all experimental patches. Plots show all K_D values determined at $+50$ mV (upper panel) and -50 mV (lower panel). Solid horizontal brackets with asterisks indicate groups significantly different from compound **1** using the Holm—Sidak method for multiple pairwise comparisons; $P < 0.01$.

The physiological concentration of free cGMP in dark-adapted rod outer segments has been estimated to be about 3.5 μM.[57,58] Given the very large fraction of closed channels, the potency for CNG channel block in the intact retina is likely to be even greater than the values reported here.

It was a concern that the amide bond in compounds **6** and **7** could be susceptible to hydrolysis by proteases; however, we found that they were resistant to both proteinase K and chymotrypsin. Chymotrypsin preferentially catalyzes the hydrolysis of peptide bonds involving L-isomers of tyrosine, phenylalanine, and tryptophan on the carboxy side.[59] As the amide bond adjacent to the aromatic ring in compounds **6** and **7** resembles a peptide bond of an aromatic amino acid residue, it was plausible that it would be recognized by the hydrophobic pocket of the chymotrypsin catalytic site. The resistance of compounds **6** and **7** to chymotrypsin may be due to the lack of a "carbon backbone" in the structure. A similar argument can be applied to explain the resistance to hydrolysis by proteinase K: the aromatic ring directly adjacent to the equivalent of a peptide bond in compounds **6** and **7** renders it unrecognizable by the endopeptidase. Not surprisingly, compounds **8** and **9** with thioamide linkages were also completely resistant to protease action.

Compound **1**'s actions are very short-lived, being rapidly degraded mainly by butyrylcholinesterase in the blood. The

greater stability of the amide and thioamide linkages should enhance the half-life. Particularly for compounds **8** and **9**, the clearance rate would likely depend on other metabolic pathways, but this would need to be determined in a proper pharmacokinetic study. One question that emerges from this study is which compound appears to have the greatest potential for clinical use? We are contemplating only local tissue uses of these compounds. Nonetheless, the stability of compounds **8** and **9** against hydrolysis is so dramatic that their safety for clinical use might come into question. The high stability of the thioamide linkage in a tetracaine-based CNG channel blocker may increase the chances for toxic systemic reactions. Large systemic doses of thiobenzamide and its para-substituted derivatives have been shown to be hepato- and nephrotoxic,[60−62] and certain thioamides such as propylthiouracil inhibit thyroid peroxidase and are used to treat hyperthyroidism.[63] These issues remain to be examined at the low doses needed to achieve CNG channel block. Lastly, compounds **7** and **9** have larger estimated $\log P$ values than compounds **6** and **8** (Table 1) and as such would theoretically have better accessibility to reach channel targets.

This study may have broader implications than for CNG channel blockers alone. There are situations in which longer lasting anesthetics are desirable, and there have been several attempts to achieve this.[64−66] The amino amide type of local anesthetics are well recognized for their better biological stability than amino esters, but the thioamide linkage, to our knowledge, is the first of its kind. Indeed, there have been some attempts to increase the half-life of **1** in biological preparations.[67−70] The hydrolysis resistant versions of **1** reported here may be attractive options for longer lasting local anesthetics; however, their effects on nerve conductance need to be further examined.

■ EXPERIMENTAL SECTION

Retinal Rod CNG Channel Expression in Oocytes. Ovaries were surgically removed from adult *Xenopus laevis* females (*Xenopus* Express; Brooksville, FL) anesthetized with ice-cold 0.1% tricaine and 0.1% $NaHCO_3$ solution. Oocytes were chemically released from ovarian follicles in Ca^{2+}-free Barth's solution (in mM: 88 NaCl, 1 KCl, 2.4 $NaHCO_3$, 0.82 $MgSO_4$, 7.5 Tris, 2.5 sodium pyruvate, 100 U/mL penicillin, and 100 μg/mL streptomycin, pH 7.4) containing 0.1 U/mL Liberase Blendzymes (Roche, Indianapolis, IN). Stages IV and V oocytes were visually sorted and stored in ND-96 (in mM: 96 NaCl, 2 KCl, 1.8 $CaCl_2$, 1 $MgCl_2$, 5 HEPES, 2.5 sodium pyruvate, 100 U/mL penicillin, and 100 μg/mL streptomycin, pH 7.4) at 16 °C. Oocytes were co-injected the following day with 33 ng of CNGA1 and 67 ng of CNGB1 cRNA (2:1) synthesized from linearized pGEM-HE expression vectors containing the channel subunit cDNA sequences[71] using T7 mMESSAGE mMACHINE (Ambion, Austin, TX). Injected oocytes were incubated at 18 °C the first day and 16 °C for the remaining days.

Electrophysiological Recordings. Recordings from inside-out excised patches were made 3−7 days after oocyte injection on an Axopatch 1D amplifier (Axon Instruments, Foster City, CA). Briefly, oocyte vitelline membranes were removed in solution containing (in mM) 200 K aspartate, 20 KCl, 1 $MgCl_2$, 10 EGTA, 10 HEPES, pH 7.4. Oocytes were placed in a recording chamber in solution containing (in mM) 130 NaCl, 2 HEPES, 0.02 EDTA, 1 EGTA, pH 7.6, and borosilicate glass electrodes (1−3 MΩ) were filled with identical solution. Macroscopic currents were filtered at 1 kHz and sampled at 2 kHz using pCLAMP 8.0 software (Axon Instruments). Channels were either fully activated with 2 mM or partially activated with 50 and 100 μM cGMP. Solutions containing different tetracaine derivatives were exchanged using a RSC-100 rapid solution changer
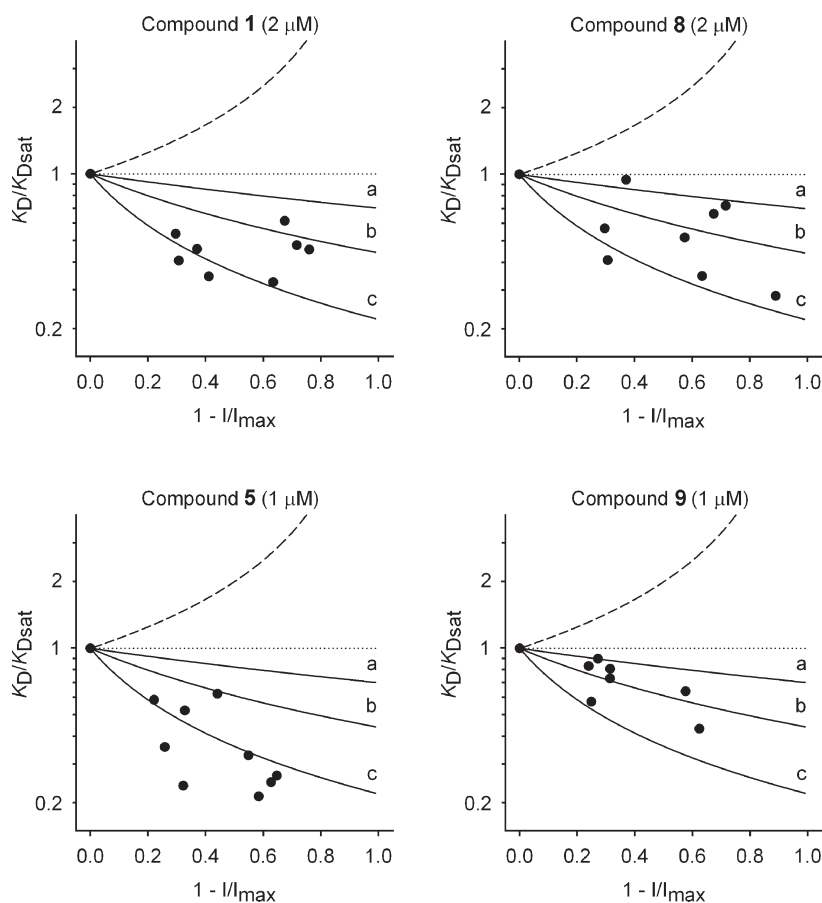
Figure 4. State dependence of block. Plots showing relationship of all K_D values determined for compounds **1** (2 μM), **8** (2 μM), **5** (1 μM), and **9** (1 μM) at subsaturating cGMP (50 or 100 μM) at +50 mV normalized to K_D values determined at saturating cGMP (2 mM), versus $1 - I/I_{max}$, which is related to the fraction of closed channels. K_D values at saturating cGMP were corrected for ion accumulation. Solid lines indicate simulations for exclusive closed channel blockers, using $K_D/K_{Dsat} = (1 - F_{sat})/(1 - F_{sat}I/I_{max})$, where F_{sat} is the estimated fraction of open heteromeric rod channels in saturating cGMP assuming $F_{sat} = 0.3$ (a),[49] 0.56 (b),[50] or 0.78 (c).[51] The dotted line is a simulation for a blocker with no preference for state, or $K_D/K_{Dsat} = 1$. The dashed line is a simulation for an exclusive open channel blocker, using $K_D/K_{Dsat} = (I/I_{max})^{-1}$.

(Molecular Kinetics, Pullman, WA). Glass syringes and Teflon tubing were used to minimize the binding of compounds to surfaces; concentrations passing through the perfusion system were verified by absorbance. Current traces were digitally filtered at 300 Hz (Gaussian) and averaged using Clampfit 8.2 software. Currents in the absence of cGMP were subtracted from all currents analyzed. K_D values were determined and expressed as the mean ± SD.

In Vitro Ester Hydrolysis. All enzymatic assays were performed with 50 μM compound in 0.1 M phosphate buffer, pH 7.4, at 37 °C with stirring, unless otherwise noted. Butyrylcholinesterase stock solutions from human serum (Sigma, St. Louis, MO) were prepared at 100 U/mL in 0.1 M phosphate buffer, pH 7.4, and stored at −20 °C until use. Compound hydrolysis was monitored on an 8452A diode array spectrophotometer (Hewlett-Packard). Product peak wavelength absorption was immediately monitored upon addition of compound. Absorbances for complete hydrolysis were determined when there were no further detectable changes. Hydrolysis rates were calculated based on the changes in absorbance during the first 1 min of hydrolysis (**1** and **5**) or first 9 min (**6** and **7**) and were adjusted to the absorbance at the completion of the reaction. All hydrolysis assays were performed in triplicate, and final rate constants are expressed as the mean ± SD of the three individually determined rate constants. In some experiments with compound **1**, samples were taken at the beginning and end of the assay to verify the hydrolysis product and the completion of the reaction by

HPLC. These samples were compared to **1** and **3** on a C18 column eluted with 0.1% TFA in water/acetonitrile.

Activity of chymotrypsin (bovine, Worthington Biochemical Co., 190 μg/mL) was verified with 90 μM 4-nitrophenyl acetate in 0.1 M HEPES solution, pH 6.5, at 37 °C with stirring. Hydrolysis product was monitored at 404 nm for 10 min. Activity of proteinase K (from *Engyodontium album*, Sigma, 165 μg/mL) was verified with 16.5 mg/mL bovine serum albumin in 0.1 M phosphate buffer, pH 7.4, at 37 °C. Samples were taken at time point increments up to 2 h when the reaction reached completion and were analyzed with 12% SDS−PAGE, stained with 0.1% Coomassie Blue.

Statistical Analysis. Statistical comparison between groups was made using a one-way repeated-measures ANOVA and the Holm−Sidak post hoc method for multiple pairwise comparisons. Statistical significance was accepted at $P < 0.01$.

Chemistry. Reagents, including **1** and **2**, were obtained from Sigma-Aldrich and were used without further purification. TLC was performed on glass backed silica plates and eluted in a mixture of 5−10% methanol and 90−95% dichloromethane. Plates were visualized using short wave UV light and KMnO$_4$. Crude compounds were initially purified using column chromatography, which was packed with normal phase silica gel and eluted using either ethyl acetate/hexane or methanol/dichloromethane mixtures. Trace impurities were removed by reversed-phase HPLC on an Xterra Prep RP8 column, 19 mm × 100 mm, 5 μm

(Waters, Milford, MA), with a water–methanol gradient (5 mM ammonium acetate, pH 5), monitored at 214 and 310 nm to yield final products. Purity was assessed to be greater than 95% with an Xterra Analytical RP8 column, 4.6 mm × 250 mm, 5 μm, under similar conditions and monitoring. ^{1}H and ^{13}C NMR spectra were obtained using a Bruker 500 MHz FT-NMR spectrometer. ESI-MS was performed on a Thermo Finnigan TSQ Classic mass spectrometer.

4-(Butylamino)benzoic Acid (3). Compound **2** (∼3 mmol) was dissolved in 15 mL of methanol with α-picoline-borane (1.1 mol equiv) and butanal (1.1 mol equiv). The mixture was stoppered with a vent needle and stirred overnight at room temperature. After 16–24 h, solvent was removed in vacuo, 10 mL 1 M HCl was added to the flask, and the mixture was stirred at room temperature for an additional 30 min. The pH was adjusted to neutral using NaHCO$_3$, and the intermediate product was extracted with ethyl acetate (2 × 60 mL). The organic layer was washed with brine (1 × 45 mL), dried with magnesium sulfate, filtered, removed in vacuo, and subsequently purified via column chromatography with 30% ethyl acetate in hexane to yield **3** (88%) as a white powder. ^{1}H NMR (500 MHz) (CD$_3$OD): δ 7.92 (d, J = 8.8 Hz, 2H), 6.55 (d, J = 8.8 Hz, 2H), 3.18 (t, J = 7.2 Hz, 2H), 1.63 (m, 2H), 1.44 (m, 2H), 0.97 (t, J = 7.4 Hz, 3H). ^{13}C NMR (125 MHz) (CD$_3$OD): δ 172.6, 153.1, 132.7, 117.3, 111.6, 43.4, 31.7, 20.5, 14.1.

4-(Octylamino)benzoic Acid (4). The product was prepared as described for **3** with octanal to yield **4** (94%) as a white powder. ^{1}H NMR (500 MHz) (CD$_3$OD): δ 7.92 (d, J = 8.9 Hz, 2H), 6.55 (d, J = 8.9 Hz, 2H), 3.17 (t, J = 7.2 Hz, 2H), 1.63 (m, 2H), 1.25–1.41 (m, 10H), 0.89 (t, J = 7.0 Hz, 3H). ^{13}C NMR (125 MHz) (CD$_3$OD): δ 172.6, 153.1, 132.7, 117.3, 111.6, 43.7, 32.1, 29.7, 29.6, 29.5, 27.4, 23.0, 14.4.

2-(Dimethylamino)ethyl 4-(Octylamino)benzoate (5). In a flame-sealed flask, **4** (∼0.50 mmol) and CDI (1.5 mol equiv) were dissolved in 3.0 mL of 1,2-dimethoxyethane (DME). The solution was stirred at 60 °C for approximately 2 h under argon. 2-(Dimethylamino)-ethanol (3 mol equiv) was added to the solution followed by a small quantity of NaH (∼2 mg). The flask was allowed to cool to room temperature and react for an additional 16–24 h. The reaction was worked up by dissolving it in 100 mL of chloroform and washing with water (2 × 60 mL) and brine (1 × 60 mL). The organic layer was dried with sodium sulfate, filtered, removed in vacuo, and subsequently purified via column chromatography with 30% ethyl acetate in hexane to yield **5** (95%) as a white powder. This compound was reported previously although synthesized by a different method.[40] ^{1}H NMR (500 MHz) (CD$_3$OD): δ 7.83 (d, J = 8.9 Hz, 2H), 6.59 (d, J = 8.7 Hz, 2H), 4.58 (t, J = 5.0 Hz, 2H), 3.57 (t, J = 5.0 Hz, 2H), 3.14 (t, J = 7.1 Hz, 2H), 3.00 (s, 6H), 1.63 (m, 2H), 1.25–1.5 (m, 10 H), 0.90 (t, J = 6.8 Hz, 3H). ^{13}C NMR (125 MHz) (CDCl$_3$): δ 166.8, 152.2, 131.6, 117.9, 111.3, 62.3, 58.0, 45.9, 43.4, 31.8, 29.4, 29.3, 29.2, 27.1, 22.7, 14.1. ESI-MS: m/z 321.1 MH$^+$. Mp: 40–41 °C.

4-(Butylamino)-N-(2-(dimethylamino)ethyl)benzamide (6). In a flame-sealed flask, **3** (∼0.50 mmol) and CDI (1.5 mol equiv) were dissolved in 3.0 mL of DME, and the mixture was stirred at 60 °C for approximately 2 h under argon. N',N'-Dimethylethane-1,2-diamine (3 mol equiv) was added to the solution followed by a small quantity of NaH (∼2 mg). The flask was allowed to cool to room temperature and react for an additional 16–24 h. The reaction was worked up by dissolving it in 100 mL of chloroform and washing with water (2 × 60 mL) and brine (1 × 60 mL). The organic layer was dried over sodium sulfate, filtered, removed in vacuo, and subsequently purified via column chromatography with 30% ethyl acetate in hexane to yield **6** (93%) as pale brown oil. ^{1}H NMR (500 MHz) (CD$_3$OD): δ 8.13 (d, J = 8.8 Hz, 2H), 7.61 (d, J = 8.8 Hz, 2H), 3.82 (t, J = 5.9 Hz, 2H), 3.44 (m, 4H), 3.02 (s, 6H), 1.76 (m, 2H), 1.50 (m, 2H), 1.02 (t, J = 7.4 Hz, 3H). ^{13}C NMR (125 MHz) (CD$_3$OD): δ 170.2, 141.8, 135.8, 131.7, 124.0, 59.5, 53.1, 44.8, 37.3, 30.3, 21.6, 14.8. ESI-MS: m/z 264.22 MH$^+$.

4-(Octylamino)-N-(2-(dimethylamino)ethyl)benzamide (7). The product was prepared as described for **6** using compound **4** to yield **7** (87%) as pale brown oil. ^{1}H NMR (500 MHz) (CDCl$_3$): δ 7.66 (d, J = 8.8 Hz, 2H), 6.99 (br, 1H), 6.55 (d, J = 8.8 Hz, 2H), 3.98 (br, 1H), 3.57 (m, 2H), 3.13 (t, J = 7.1 Hz, 2H), 2.68 (t, J = 5.7 Hz, 2H), 2.40 (s, 6H), 1.61 (m, 2H), 1.25–1.40 (m, 10H), 0.88 (t, J = 6.9 Hz, 3H). ^{13}C NMR (125 MHz) (CDCl$_3$): δ 167.8, 151.4, 129.1, 122.4, 111.8, 58.4, 51.1, 45.2, 43.8, 36.9, 32.1, 29.7, 29.6, 27.4, 23.0, 14.4. ESI-MS: m/z 320.08 MH$^+$.

4-(Butylamino)-N-(2-(dimethylamino)ethyl)benzothioamide (8). In a flame-sealed flask, **6** (∼0.25 mmol) was dissolved in 5 mL of dry toluene with Lawesson's reagent (1 mol equiv) and refluxed under argon for 2.5 h. The mixture was dissolved in 20 mL of ethyl acetate, washed with water (2 × 20 mL), dried over sodium sulfate, and subsequently purified via column chromatography with 10% methanol in dichloromethane to yield **8** (26%) as yellow oil. ^{1}H NMR (500 MHz) (CDCl$_3$): δ 8.64 (br, 1H), 7.79 (d, J = 9 Hz, 2H), 6.51 (d, J = 9 Hz, 2H), 4.03 (br, 1H), 3.97 (m, 2H), 3.14 (t, J = 7.1 Hz, 2H), 2.85 (m, 2H), 2.44 (s, 6H), 1.60 (m, 2H), 1.42 (m, 2H), 0.96 (t, J = 7.4 Hz, 3H). ^{13}C NMR (125 MHz) (CDCl$_3$): δ 197.6, 151.7, 129.3, 129.2, 111.7, 57.0, 45.1, 43.5, 43.2, 31.7, 20.5, 14.2. ESI-MS: m/z 280.1 MH$^+$.

4-(Octylamino)-N-(2-(dimethylamino)ethyl)benzothioamide (9). The product was prepared as described for **8** using compound **7** to yield **9** (73%) as yellow oil. ^{1}H NMR (500 MHz) (CDCl$_3$): δ 8.41 (br, 1H), 7.76 (d, J = 8.8 Hz, 2H), 6.52 (d, J = 8.8 Hz, 2H), 4.02 (br, 1H), 3.90 (m, 2H), 3.14 (t, J = 7.1 Hz, 2H), 2.72 (t, J = 5.4 Hz, 2H), 2.35 (s, 6H), 1.62 (m, 2H), 1.25–1.40 (m, 10H), 0.88 (t, J = 7.0 Hz, 3H). ^{13}C NMR (125 MHz) (CDCl$_3$): δ 197.4, 151.6, 129.4, 129.2, 111.8, 56.9, 51.2, 45.2, 43.8, 43.6, 32.2, 29.7, 29.6, 27.4, 23.0, 14.5. ESI-MS: m/z 336.13 MH$^+$.

■ **AUTHOR INFORMATION**

Corresponding Author
*Phone: 503-494-7463. Fax: 503-494-4352. E-mail: karpenj@oh-su.edu.

■ **ABBREVIATIONS USED**

CDI, 1,1′-carbonyldiimidazole; CNG, cyclic nucleotide-gated; DME, 1,2-dimethoxyethane

■ **REFERENCES**

(1) Fesenko, E. E.; Kolesnikov, S. S.; Lyubarsky, A. L. Induction by cyclic GMP of cationic conductance in plasma membrane of retinal rod outer segment. *Nature* **1985**, *313*, 310–313.

(2) Nakamura, T.; Gold, G. H. A cyclic nucleotide-gated conductance in olfactory receptor cilia. *Nature* **1987**, *325*, 442–444.

(3) Kuzmiski, J. B.; MacVicar, B. A. Cyclic nucleotide-gated channels contribute to the cholinergic plateau potential in hippocampal CA1 pyramidal neurons. *J. Neurosci.* **2001**, *21*, 8707–8714.

(4) Parent, A.; Schrader, K.; Munger, S. D.; Reed, R. R.; Linden, D. J.; Ronnett, G. V. Synaptic transmission and hippocampal long-term potentiation in olfactory cyclic nucleotide-gated channel type 1 null mouse. *J. Neurophysiol.* **1998**, *79*, 3295–3301.

(5) Kaupp, U. B.; Seifert, R. Cyclic nucleotide-gated ion channels. *Physiol. Rev.* **2002**, *82*, 769–824.

(6) Matulef, K.; Zagotta, W. N. Cyclic nucleotide-gated ion channels. *Annu. Rev. Cell Dev. Biol.* **2003**, *19*, 23–44.

(7) Biel, M.; Michalakis, S. Cyclic nucleotide-gated channels. *Handb. Exp. Pharmacol.* **2009**, *191*, 111–136.

(8) Farber, D. B.; Lolley, R. N. Light-induced reduction in cyclic GMP of retinal photoreceptor cells in vivo: abnormalities in the degenerative diseases of RCS rats and rd mice. *J. Neurochem.* **1977**, *28*, 1089–1095.

(9) Bowes, C.; Li, T.; Danciger, M.; Baxter, L. C.; Applebury, M. L.; Farber, D. B. Retinal degeneration in the rd mouse is caused by a defect in the beta subunit of rod cGMP-phosphodiesterase. *Nature* **1990**, *347*, 677–680.

(10) Pierce, E. A. Pathways to photoreceptor cell death in inherited retinal degenerations. *BioEssays* **2001**, *23*, 605–618.

(11) Pacione, L. R.; Szego, M. J.; Ikeda, S.; Nishina, P. M.; McInnes, R. R. Progress toward understanding the genetic and biochemical mechanisms of inherited photoreceptor degenerations. *Annu. Rev. Neurosci.* **2003**, *26*, 657–700.

(12) Olshevskaya, E. V.; Calvert, P. D.; Woodruff, M. L.; Peshenko, I. V.; Savchenko, A. B.; Makino, C. L.; Ho, Y. S.; Fain, G. L.; Dizhoor, A. M. The Y99C mutation in guanylyl cyclase-activating protein 1 increases intracellular Ca^{2+} and causes photoreceptor degeneration in transgenic mice. *J. Neurosci.* **2004**, *24*, 6078–6085.

(13) Nishiguchi, K. M.; Sokal, I.; Yang, L.; Roychowdhury, N.; Palczewski, K.; Berson, E. L.; Dryja, T. P.; Baehr, W. A novel mutation (I143NT) in guanylate cyclase-activating protein 1 (GCAP1) associated with autosomal dominant cone degeneration. *Invest. Ophthalmol. Visual Sci.* **2004**, *45*, 3863–3870.

(14) Trifunovic, D.; Dengler, K.; Michalakis, S.; Zrenner, E.; Wissinger, B.; Paquet-Durand, F. cGMP-dependent cone photoreceptor degeneration in the cpfl1 mouse retina. *J. Comp. Neurol.* **2010**, *518*, 3604–3617.

(15) He, L.; Poblenz, A. T.; Medrano, C. J.; Fox, D. A. Lead and calcium produce rod photoreceptor cell apoptosis by opening the mitochondrial permeability transition pore. *J. Biol. Chem.* **2000**, *275*, 12175–12184.

(16) Rohrer, B.; Pinto, F. R.; Hulse, K. E.; Lohr, H. R.; Zhang, L.; Almeida, J. S. Multidestructive pathways triggered in photoreceptor cell death of the rd mouse as determined through gene expression profiling. *J. Biol. Chem.* **2004**, *279*, 41903–41910.

(17) Doonan, F.; Donovan, M.; Cotter, T. G. Activation of multiple pathways during photoreceptor apoptosis in the rd mouse. *Invest. Ophthalmol. Visual Sci.* **2005**, *46*, 3530–3538.

(18) Fox, D. A.; Poblenz, A. T.; He, L.; Harris, J. B.; Medrano, C. J. Pharmacological strategies to block rod photoreceptor apoptosis caused by calcium overload: a mechanistic target-site approach to neuroprotection. *Eur. J. Ophthalmol.* **2003**, *13* (Suppl. 3), S44–S56.

(19) Paquet-Durand, F.; Beck, S.; Michalakis, S.; Goldmann, T.; Huber, G.; Muhlfriedel, R.; Trifunovic, D.; Fischer, M. D.; Fahl, E.; Duetsch, G.; Becirovic, E.; Wolfrum, U.; van Veen, T.; Biel, M.; Tanimoto, N.; Seeliger, M. W. A key role for cyclic nucleotide gated (CNG) channels in cGMP-related retinitis pigmentosa. *Hum. Mol. Genet.* **2011**, *20*, 941–1472.

(20) Vallazza-Deschamps, G.; Cia, D.; Gong, J.; Jellali, A.; Duboc, A.; Forster, V.; Sahel, J. A.; Tessier, L. H.; Picaud, S. Excessive activation of cyclic nucleotide-gated channels contributes to neuronal degeneration of photoreceptors. *Eur. J. Neurosci.* **2005**, *22*, 1013–1022.

(21) Woodruff, M. L.; Olshevskaya, E. V.; Savchenko, A. B.; Peshenko, I. V.; Barrett, R.; Bush, R. A.; Sieving, P. A.; Fain, G. L.; Dizhoor, A. M. Constitutive excitation by Gly90Asp rhodopsin rescues rods from degeneration caused by elevated production of cGMP in the dark. *J. Neurosci.* **2007**, *27*, 8805–8815.

(22) Liu, X.; Pawlyk, B. S.; Adamian, M.; Olshevskaya, E. V.; Dizhoor, A. M.; Makino, C. L.; Li, T. Increased light exposure alleviates one form of photoreceptor degeneration marked by elevated calcium in the dark. *PLoS One* **2009**, *4*, e8438.

(23) Brown, R. L.; Strassmaier, T.; Brady, J. D.; Karpen, J. W. The pharmacology of cyclic nucleotide-gated channels: emerging from the darkness. *Curr. Pharm. Des.* **2006**, *12*, 3597–3613.

(24) Stern, J. H.; Kaupp, U. B.; MacLeish, P. R. Control of the light-regulated current in rod photoreceptors by cyclic GMP, calcium, and l-cis-diltiazem. *Proc. Natl. Acad. Sci. U.S.A.* **1986**, *83*, 1163–1167.

(25) Hashimoto, Y.; Yabana, H.; Murata, S. Electrophysiological effect of l-cis-diltiazem, the stereoisomer of d-cis-diltiazem, on isolated guinea-pig left ventricular myocytes. *Eur. J. Pharmacol.* **2000**, *391*, 217–223.

(26) Haynes, L. W. Block of the cyclic GMP-gated channel of vertebrate rod and cone photoreceptors by l-cis-diltiazem. *J. Gen. Physiol.* **1992**, *100*, 783–801.

(27) Galizzi, J. P.; Borsotto, M.; Barhanin, J.; Fosset, M.; Lazdunski, M. Characterization and photoaffinity labeling of receptor sites for the Ca^{2+} channel inhibitors d-cis-diltiazem, (+/−)-bepridil, desmethoxy-verapamil, and (+)-PN 200-110 in skeletal muscle transverse tubule membranes. *J. Biol. Chem.* **1986**, *261*, 1393–1397.

(28) Quandt, F. N.; Nicol, G. D.; Schnetkamp, P. P. Voltage-dependent gating and block of the cyclic-GMP-dependent current in bovine rod outer segments. *Neuroscience* **1991**, *42*, 629–638.

(29) Schnetkamp, P. P. Sodium ions selectively eliminate the fast component of guanosine cyclic $3',5'$-phosphate induced Ca^{2+} release from bovine rod outer segment disks. *Biochemistry* **1987**, *26*, 3249–3253.

(30) Schnetkamp, P. P. Cation selectivity of and cation binding to the cGMP-dependent channel in bovine rod outer segment membranes. *J. Gen. Physiol.* **1990**, *96*, 517–534.

(31) Sunami, A.; Dudley, S. C., Jr.; Fozzard, H. A. Sodium channel selectivity filter regulates antiarrhythmic drug binding. *Proc. Natl. Acad. Sci. U.S.A.* **1997**, *94*, 14126–14131.

(32) Ragsdale, D. S.; McPhee, J. C.; Scheuer, T.; Catterall, W. A. Molecular determinants of state-dependent block of Na^+ channels by local anesthetics. *Science* **1994**, *265*, 1724–1728.

(33) Ragsdale, D. S.; McPhee, J. C.; Scheuer, T.; Catterall, W. A. Common molecular determinants of local anesthetic, antiarrhythmic, and anticonvulsant block of voltage-gated Na^+ channels. *Proc. Natl. Acad. Sci. U.S.A.* **1996**, *93*, 9270–9275.

(34) Catterall, W. A. Molecular mechanisms of gating and drug block of sodium channels. *Novartis Found. Symp.* **2002**, *241*, 206–218.

(35) Fodor, A. A.; Black, K. D.; Zagotta, W. N. Tetracaine reports a conformational change in the pore of cyclic nucleotide-gated channels. *J. Gen. Physiol.* **1997**, *110*, 591–600.

(36) Hille, B. Local anesthetics: hydrophilic and hydrophobic pathways for the drug—receptor reaction. *J. Gen. Physiol.* **1977**, *69*, 497–515.

(37) Fodor, A. A.; Gordon, S. E.; Zagotta, W. N. Mechanism of tetracaine block of cyclic nucleotide-gated channels. *J. Gen. Physiol.* **1997**, *109*, 3–14.

(38) Ghatpande, A. S.; Uma, R.; Karpen, J. W. A multiply charged tetracaine derivative blocks cyclic nucleotide-gated channels at subnanomolar concentrations. *Biochemistry* **2003**, *42*, 265–270.

(39) Strassmaier, T.; Uma, R.; Ghatpande, A. S.; Bandyopadhyay, T.; Schaffer, M.; Witte, J.; McDougal, P. G.; Brown, R. L.; Karpen, J. W. Modifications to the tetracaine scaffold produce cyclic nucleotide-gated channel blockers with widely varying efficacies. *J. Med. Chem.* **2005**, *48*, 5805–5812.

(40) Strassmaier, T.; Kirk, S. R.; Banerji, T.; Karpen, J. W. Block of cyclic nucleotide-gated channels by tetracaine derivatives: role of apolar interactions at two distinct locations. *Bioorg. Med. Chem. Lett.* **2008**, *18*, 645–649.

(41) Fichman, R. A. Use of topical anesthesia alone in cataract surgery. *J. Cataract Refractive Surg.* **1996**, *22*, 612–614.

(42) Amiel, H.; Koch, P. S. Tetracaine hydrochloride 0.5% versus lidocaine 2% jelly as a topical anesthetic agent in cataract surgery: comparative clinical trial. *J. Cataract Refractive Surg.* **2007**, *33*, 98–100.

(43) Kalow, W. Hydrolysis of local anesthetics by human serum cholinesterase. *J. Pharmacol. Exp. Ther.* **1952**, *104*, 122–134.

(44) Sato, S.; Sakamoto, T.; Miyazawa, E.; Kikugawa, Y. One-pot reductive amination of aldehydes and ketones with [alpha]-picoline-borane in methanol, in water, and in neat conditions. *Tetrahedron* **2004**, *60*, 7899–7906.

(45) Staab, H. A. New methods of preparative organic chemistry IV. Syntheses using heterocyclic amides (azolides). *Angew. Chem., Int. Ed. Engl.* **1962**, *1*, 351–367.

(46) Ozturk, T.; Ertas, E.; Mert, O. Use of Lawesson's reagent in organic syntheses. *Chem. Rev.* **2007**, *107*, 5210–5278.

(47) Korschen, H. G.; Illing, M.; Seifert, R.; Sesti, F.; Williams, A.; Gotzes, S.; Colville, C.; Muller, F.; Dose, A.; Godde, M.; Molday, L.; Kaupp, U. B.; Molday, R. S. A 240 kDa protein represents the complete beta subunit of the cyclic nucleotide-gated channel from rod photoreceptor. *Neuron* **1995**, *15*, 627–636.

(48) Zimmerman, A. L.; Karpen, J. W.; Baylor, D. A. Hindered diffusion in excised membrane patches from retinal rod outer segments. *Biophys. J.* **1988**, *54*, 351–355.

(49) Matthews, G.; Watanabe, S. Activation of single ion channels from toad retinal rod inner segments by cyclic GMP: concentration dependence. *J. Physiol.* **1988**, *403*, 389–405.

(50) Taylor, W. R.; Baylor, D. A. Conductance and kinetics of single cGMP-activated channels in salamander rod outer segments. *J. Physiol.* **1995**, *483* (Part 3), 567–582.

(51) Bucossi, G.; Nizzari, M.; Torre, V. Single-channel properties of ionic channels gated by cyclic nucleotides. *Biophys. J.* **1997**, *72*, 1165–1181.

(52) Leopold, I. H. Autonomic drugs and their influence on chorioidal vessel caliber. *Trans. Am. Ophthalmol. Soc.* **1951**, *49*, 625–672.

(53) Sanchez-Chavez, G.; Vidal, C. J.; Salceda, R. Acetyl- and butyrylcholinesterase activities in the rat retina and retinal pigment epithelium. *J. Neurosci. Res.* **1995**, *41*, 655–662.

(54) Lee, V. H.; Chang, S. C.; Oshiro, C. M.; Smith, R. E. Ocular esterase composition in albino and pigmented rabbits: possible implications in ocular prodrug design and evaluation. *Curr. Eye Res.* **1985**, *4*, 1117–1125.

(55) Stratford, R. E., Jr.; Lee, V. H. Ocular aminopeptidase activity and distribution in the albino rabbit. *Curr. Eye Res.* **1985**, *4*, 995–999.

(56) Stratford, R. E., Jr.; Lee, V. H. Aminopeptidase activity in albino rabbit extraocular tissues relative to the small intestine. *J. Pharm. Sci.* **1985**, *74*, 731–734.

(57) Cote, R. H.; Brunnock, M. A. Intracellular cGMP concentration in rod photoreceptors is regulated by binding to high and moderate affinity cGMP binding sites. *J. Biol. Chem.* **1993**, *268*, 17190–17198.

(58) Yau, K. W.; Nakatani, K. Light-suppressible, cyclic GMP-sensitive conductance in the plasma membrane of a truncated rod outer segment. *Nature* **1985**, *317*, 252–255.

(59) Appel, W. Chymotrypsin: molecular and catalytic properties. *Clin. Biochem.* **1986**, *19*, 317–322.

(60) Traiger, G. J.; Gammal, L. M.; Cox, D. N.; Haschek, W. M. Nephrotoxicity of para-substituted thiobenzamide derivatives in the rat. *Toxicology* **1989**, *58*, 43–56.

(61) Grossman, S. J.; Patrick, D. H.; Kornbrust, D.; Smith, P. F.; Herold, E. G.; DeLuca, J. G.; Zacchei, A. G. Thiobenzamide-induced hepatotoxicity: effects of substituents and route of administration on the nature and extent of liver injury. *Toxicol. Appl. Pharmacol.* **1991**, *111*, 388–408.

(62) Ikehata, K.; Duzhak, T. G.; Galeva, N. A.; Ji, T.; Koen, Y. M.; Hanzlik, R. P. Protein targets of reactive metabolites of thiobenzamide in rat liver in vivo. *Chem. Res. Toxicol.* **2008**, *21*, 1432–1442.

(63) Nagasaka, A.; Hidaka, H. Effect of antithyroid agents 6-propyl-2-thiouracil and 1-methyl-2-mercaptoimidazole on human thyroid iodine peroxidase. *J. Clin. Endocrinol. Metab.* **1976**, *43*, 152–158.

(64) Mannheimer, W.; Pizzolato, P.; Adriani, J. Mode of action and effects on tissues of long-acting local anesthetics. *JAMA, J. Am. Med. Assoc.* **1954**, *154*, 29–32.

(65) Epstein-Barash, H.; Shichor, I.; Kwon, A. H.; Hall, S.; Lawlor, M. W.; Langer, R.; Kohane, D. S. Prolonged duration local anesthesia with minimal toxicity. *Proc. Natl. Acad. Sci. U.S.A.* **2009**, *106*, 7125–7130.

(66) Ivani, G.; Borghi, B.; van Oven, H. Levobupivacaine. *Minerva Anestesiol.* **2001**, *67*, 20–23.

(67) Boedeker, B. H.; Lojeski, E. W.; Kline, M. D.; Haynes, D. H. Ultra-long-duration local anesthesia produced by injection of lecithin-coated tetracaine microcrystals. *J. Clin. Pharmacol.* **1994**, *34*, 699–702.

(68) Fisher, R.; Hung, O.; Mezei, M.; Stewart, R. Topical anaesthesia of intact skin: liposome-encapsulated tetracaine vs EMLA. *Br. J. Anaesth.* **1998**, *81*, 972–973.

(69) Wang, G. K.; Vladimirov, M.; Shi, H.; Mok, W. M.; Thalhammer, J. G.; Anthony, D. C. Structure–activity relation of *N*-alkyl tetracaine derivatives as neurolytic agents for sciatic nerve lesions. *Anesthesiology* **1998**, *88*, 417–428.

(70) Kissin, I.; Lee, S. S.; Bradley, E. L., Jr. Hyperalgesia caused by nerve transection: long-lasting block prevents early hyperalgesia in the receptive field of the surviving nerve. *Anesth. Analg.* **1999**, *89*, 1475–1481.

(71) Strassmaier, T.; Karpen, J. W. Novel N7- and N1-substituted cGMP derivatives are potent activators of cyclic nucleotide-gated channels. *J. Med. Chem.* **2007**, *50*, 4186–4194.